Published in final edited form as:
Neuroimage. 2014 February 1; 86: 461–469. doi:10.1016/j.neuroimage.2013.10.043.

Lateralized parietotemporal oscillatory phase synchronization during auditory selective attention

Samantha Huang[1], **Wei-Tang Chang**[1], **John W. Belliveau**[1,2], **Matti Hämäläinen**[1,2], and **Jyrki Ahveninen**[1]

[1]Harvard Medical School – Athinoula A. Martinos Center for Biomedical Imaging, Department of Radiology, Massachusetts General Hospital, Charlestown, MA, USA

[2]Harvard-MIT Division of Health Sciences and Technology, Cambridge, MA, USA

Abstract

Based on the infamous left-lateralized neglect syndrome, one might hypothesize that the dominating right parietal cortex has a bilateral representation of space, whereas the left parietal cortex represents only the contralateral right hemispace. Whether this principle applies to human auditory attention is not yet fully clear. Here, we explicitly tested the differences in cross-hemispheric functional coupling between the intraparietal sulcus (IPS) and auditory cortex (AC) using combined magnetoencephalography (MEG), EEG, and functional MRI (fMRI). Inter-regional pairwise phase consistency (PPC) was analyzed from data obtained during dichotic auditory selective attention task, where subjects were in 10-s trials cued to attend to sounds presented to one ear and to ignore sounds presented in the opposite ear. Using MEG/EEG/fMRI source modeling, parietotemporal PPC patterns were (**a**) mapped between all AC locations vs. IPS seeds and (**b**) analyzed between four anatomically defined AC regions-of-interest (ROI) vs. IPS seeds. Consistent with our hypothesis, stronger cross-hemispheric PPC was observed between the right IPS and left AC for attended right-ear sounds, as compared to PPC between the left IPS and right AC for attended left-ear sounds. In the mapping analyses, these differences emerged at 7–13 Hz, i.e., at the theta to alpha frequency bands, and peaked in Heschl's gyrus and lateral posterior non-primary ACs. The ROI analysis revealed similarly lateralized differences also in the beta and lower theta bands. Taken together, our results support the view that the right parietal cortex dominates auditory spatial attention.

1. Introduction

Many studies have documented modulations of ACs when a human subject pays attention to sounds originating in one location of space and when he/she actively ignores other sources (Ahveninen et al., 2011; Alho et al., 2003; Grady et al., 1997; Hansen and Hillyard, 1980; Hillyard et al., 1973; Petkov et al., 2004; Woldorff et al., 1998; Zatorre et al., 1999). These modulations are presumably driven by an executive network of frontoparietal cortex regions (Huang et al., 2012; Mayer et al., 2009; Mayer et al., 2006; Shomstein and Yantis, 2004, 2006; Wu et al., 2007). An association area specifically linked to the spatial domain of

Corresponding Author: Jyrki Ahveninen, Ph.D., MGH/MIT/HMS-Martinos Center, Bldg. 149 13th Street, Charlestown MA 02129, phone (617) 726-6584; fax (617) 726-7422, jyrki@nmr.mgh.harvard.edu.

auditory attention is the posterior parietal cortex, which is reportedly activated during a great variety of tasks that require orienting and focusing of attention to relevant locations of acoustic environment (Ahveninen et al., 2012; Ahveninen et al., 2006; Alho et al., 2003; Huang et al., 2012; Kong et al., 2012; Mayer et al., 2009; Mayer et al., 2006; Santangelo et al., 2009; Shomstein and Yantis, 2004, 2006; Wu et al., 2007; Zatorre et al., 1999). Exactly how the executive posterior parietal cortices and the AC areas that process initial stimulus representations work together to enable spatial attention remains unknown.

In contrast to vision, the auditory system lacks a straightforward correspondence between specific spatial locations and sensory receptive fields. Even the most fundamental principles concerning the hemispheric lateralization of spatial representations, which have been clearly demonstrated in visual and somatosensory systems, are still elusive in the auditory domain. Whereas data from animal lesion models (Jenkins and Masterton, 1982), human neurological patients (Sanchez-Longo and Forster, 1958), and certain human neuroimaging studies (Alho et al., 1999) support a contra-lateralized attention effect, there is also a profusion of evidence for right-hemispheric dominance of auditory spatial processing, both at the level of ACs (Baumgart et al., 1999; Hart et al., 2004; Kaiser et al., 2000; Krumbholz et al., 2005; Palomäki et al., 2005; Salminen et al., 2010; Tiitinen et al., 2006) and higher-order posterior parietal regions (Griffiths et al., 1998; Zatorre et al., 1999). Further, certain neuropsychological studies in patients with brain lesions have suggested that the right parieto-temporal cortices include a global representation of auditory space (Bisiach et al., 1984; Ruff et al., 1981; Zatorre and Penhune, 2001). However, there is also evidence supporting a "neglect model" (Teshiba et al., 2012), coined based on the hemispatial inattention syndrome in right-handed patients with right posterior parietal lesions. This model predicts that the right parietal cortex controls auditory attention to both hemifields and that the left posterior parietal cortex has a representation for the contralateral right hemifield of the acoustic space only. Evidence consistent with this idea has been found in studies on auditory perceptual deficits in human neurological patients (Spierer et al., 2009; Tanaka et al., 1999), as well as in auditory transcranial magnetic stimulation (TMS) experiments in healthy human subjects (At et al., 2011). A recent fMRI study utilizing resting-state functional connectivity analyses, further, suggested that the "neglect model" might apply on the attentional modulation patterns of posterior non-primary AC areas (Teshiba et al., 2012). Interestingly, the TMS studies by At and colleagues (At et al., 2011) observed two distinct temporal effects. TMS manipulations at very early latencies resulted in a contralateral localization deficits, while TMS manipulations to the right parietal cortex at later latencies resulted in a generalized localization deficit. However, to our knowledge, very few previous neuroimaging studies have investigated how the functional connectivity between parietal regions and ACs evolves temporally after sound presentation.

Functional coupling between distant brain areas can be studied by analyzing collective rhythmic activation patterns referred to as neuronal oscillations (Jensen et al., 2007; Kopell et al., 2000; Singer, 1999; Varela et al., 2001; Womelsdorf and Fries, 2007). Accumulating evidence suggests that long-range synchronization of neuronal oscillations plays a crucial role for attention and cognitive control (Jensen et al., 2007; Womelsdorf and Fries, 2007). Such long-range synchronization across brain regions can be explicitly quantified based on phase locking of oscillatory activities of distant groups of neurons at different frequency ranges. While it is well-documented that the high-frequency gamma-band (30–100 Hz) oscillations are involved in synchronizing the activity of local groups of neurons (Varela et al., 2001) and enhancing the stimulus representations from bottom-up to higher-order processing areas (Buschman and Miller, 2007), lower-frequency (<30 Hz) oscillations that have more robust spike timing delays might be better suited for a longer-range coupling mechanism associated with the “broadcast” of top-down signals (Engel et al., 2001; Ermentrout and Kopell, 1998; Kopell et al., 2000; von Stein and Sarnthein, 2000). There is

evidence of long-range oscillatory coupling of neuronal networks at the 4–7 Hz theta (Harris et al., 2002; Jensen, 2001) and 7–15 Hz alpha (Palva and Palva, 2007) ranges. EEG source-localization studies have demonstrated increased long-range theta and alpha phase locking during working memory processing (Schack et al., 2005), and increased frontoparietal theta phase locking during execution of novel finger movements (Sauseng et al., 2007). Recent EEG studies also suggest that theta-band coherence across different electrode sites increases during cognitive conflict processing (Moore et al., 2006). Meanwhile, there is modeling (Kopell et al., 2000) and experimental (Roelfsema et al., 1997; von Stein et al., 2000) evidence that beta-band (15–30 Hz) oscillations organize synchronization between distant neuronal sites. For example, extracellular measurements in the cat brain have shown that inter-regional beta-frequency synchronization increases during tasks requiring attention and cognitive control (Roelfsema et al., 1997; von Stein et al., 2000). Similarly, a recent MEG study suggested that frontal-parietaltemporal attentional networks communicate via transient long-range phase synchronization at the beta band (Gross et al., 2004).

Within the posterior parietal cortices, neurons associated with voluntary auditory spatial processing have, specifically, been found in the intraparietal sulcus (IPS). According to neurophysiological studies in non-human primates, subareas of IPS may include modality-specific neurons processing auditory space (Cohen et al., 2005). Recent MEG studies using paired directed coherence (PDC) measures of effective connectivity analyses suggested that a time-varying connectivity pattern of the right AC to the right IPS underlie cued spatial auditory attention (Weisz et al., 2013), consistent with an idea that the right IPS plays a major role in voluntary auditory spatial attention. However, few studies have compared functional coupling between right and left parietal regions and ACs. Here, we used combined MEG/EEG/fMRI to compare phase locking between contralateral vs. ipsilateral IPS and superior temporal AC areas during auditory spatial selective attention. It has been well documented that sounds presented to one ear create the strongest response in the hemisphere contralateral to the stimulated ear (*e.g.*, Langers et al., 2007; Virtanen et al., 2007; Woods et al., 2009). Particularly in the case of MEG/EEG responses, this phenomenon allows for spatiotemporal tagging of activities to separate attended vs. ignored sound events. Our specific purpose was to compare phase locking patterns between the right vs. left IPS and ACs contralateral to the attended vs. ignored ear. As predicted by the "neglect model", our underlying assumption was that the left IPS would have a more lateralized connectivity pattern to auditory areas representing the task relevant sound, and that it would only process sound presented to the right auditory hemifield (i.e., here, to the right ear). The right IPS, in contrast, was presumed to contain a bilateral representation of the auditory space (i.e., it was presumed to regulate attention to sounds presented to both ears). Finally, we presumed that parietotemporal attentional functional connectivity patterns could be modeled by comparing oscillatory theta-to-beta range phase locking between each IPS and AC areas contralateral to the attended ear.

Our specific hypothesis, based on the "neglect model", was that the phase locking between right IPS and left auditory areas presenting task-relevant sounds in an attend-right-ear condition must be significantly stronger than the phase locking between the left IPS and right AC areas representing task-relevant sounds during an attend-left-ear condition (Figure 1). To test this hypothesis, we applied fMRI-informed cortically-constrained MEG/EEG source modeling of oscillatory activities (Ahveninen et al., 2011; Ahveninen et al., 2012; Lin et al., 2004) and surface-based anatomical registration methods that align cortical folding patterns across both subject and hemisphere (Greve et al., 2013).

2. Material and Methods

2.1. Task and stimuli

During MEG/EEG and fMRI acquisitions, subjects (*N*=16, mean ± SD age = 23 ± 5 years, 8 females) were presented with 10-second dichotic listening trials (Figure 2). At the onset of each trial, subjects started hearing, in a random order, 800-Hz pure tones in the right ear and 1500-Hz pure tones in the left ear (duration 50 ms, 5-ms ramps), at a stimulus onset asynchrony (SOA) of 350–750 ms. The subjects were instructed to look at a fixation mark and wait for a monaural cue (250-ms buzzer sound). Upon hearing the cue, they were advised to shift and engage attention to sounds presented to the cued, ear, and to discriminate a target stimulus (monaural two-tone complex with 800- and 1500-Hz components, 50-ms duration, 5-ms ramps) that was embedded within the standard-sound sequence in 40% of the trials. Of the remaining trials, 20% consisted of only standard sounds, 20% included a cue but no target, and 20% included a cue but the target was replaced by a task-irrelevant novel sound in the uncued ear. Our analysis concentrated on the comparisons on phase-locking patterns elicited after the first two standard sounds presented after each cue, occurring before the potential target (or other task-irrelevant sounds), which were in each trial, randomly, either task relevant or irrelevant. The average interval between the cue and the target was 1.7 s. The responses related to attention cues, targets, and novels have been analyzed and reported separately (Ahveninen et al., 2013). There was always a period of at least 650 ms after the cue onset, to allow the subject to engage attention to the designated ear before the subsequent standard sound.

The trials were separated by an auditory signal (the sound of fMRI acquisition or a corresponding recording during MEG/EEG; duration 2.18 s). In all sessions, sound stimuli were presented at 55 dB over the subjective hearing threshold, tested individually at the beginning of each session for each ear. In each trial, auditory stimuli started 2.3 s after the onset of preceding scan/simulation and ending on average 1.3 s before the next scan. During fMRI, three silent baseline trials occurred after every 6 active trials (i.e., a mixed blocked/event-related design was utilized). The task was taught to the subjects using a standardized computerized approach taking about 5 minutes before measurements. Individual trials with target-detection responses beyond the subject's mean ± 2SD reaction time (RT) were considered outliers. One subject was excluded from the final MEG/EEG/fMRI analyses because of an incapability to perform the tasks and three other subjects for technical reasons from an initial group of 20 subjects.

2.2. Data acquisition

Human subjects' approval was obtained and voluntary consents were signed before each measurement. We recorded 306-channel MEG (Elekta-Neuromag, Helsinki, Finland) and 74-channel EEG data simultaneously in a magnetically shielded room (sampling rate 600 Hz, passband 0.01–192 Hz). The average reference was utilized for all analyses of EEG data. The position of the head relative to the MEG sensor array was monitored continuously using four Head-Position Indicator (HPI) coils attached to the scalp. Electro-oculogram (EOG) was also recorded to monitor eye artifacts. Whole-head 3T fMRI was acquired in a separate session using a 32-channel coil (Siemens TimTrio, Erlagen, Germany). A sparse-sampling gradient-echo BOLD sequence (TR/TE = 10,000/30 ms, 7.82-s silent period between acquisitions, flip angle 90°, FOV 192 mm) with 36 axial slices aligned along the anterior-posterior commissure line (3-mm slices, including 0.75-mm gap, 3×3 mm^2 in-plane resolution), with the coolant pump switched off, was utilized to circumvent response contamination by scanner noise. T1-weighted structural MRIs were obtained for combining anatomical and functional data using a multi-echo MPRAGE pulse sequence (TR=2510 ms; 4 echoes with TEs = 1.64 ms, 3.5 ms, 5.36 ms, 7.22 ms; 176 sagittal slices with 1×1×1 mm^3

voxels, 256×256 mm^2 matrix; flip angle = 7°). A field mapping sequence (TR= 500 ms, flip angle 55°; TE1=2.83 ms, TE2=5.29 ms) with similar slice and voxel parameters to the EPI sequence was utilized to obtain phase and magnitude maps utilized for unwarping of B_0 distortions of the functional data.

2.3. Data analysis

Neuronal bases of auditory attention shifting were studied using an MEG/EEG/fMRI approach (Ahveninen et al., 2011; Dale et al., 2000). External MEG noise was suppressed and subject movements, estimated continuously at 200-ms intervals, were compensated for using the signal-space separation method (Taulu et al., 2005) (Maxfilter, Elekta-Neuromag, Helsinki, Finland). The MEG/EEG data were downsampled (300 samples/s, passband 0.5–100 Hz). Epochs coinciding with over 150 μV EOG, 100 μV EEG, 2 pT/cm MEG gradiometer, or 5 pT MEG magnetometer peak-to-peak signals were excluded from further analyses. A signal-space projection (SSP), calculated around the time points of artifacts, was used for removing MEG/EEG field patterns originating from the eyes.

To calculate fMRI-guided depth-weighted ℓ_2 minimum-norm estimates (MNE) (Hämäläinen et al., 1993; Lin et al., 2006), the information from structural segmentation of the individual MRIs and the MEG sensor and EEG electrode locations were used to compute the forward solutions for all putative source locations in the cortex using a three-compartment boundary element model (Hämäläinen et al., 1993). The shapes of the surfaces separating the scalp, skull, and brain compartments were determined from the anatomical MRI data using FreeSurfer 5.0 (http://surfer.nmr.mgh.harvard.edu/). For inverse computations, cortical surfaces extracted with FreeSurfer were decimated to ~1,000 vertices per hemisphere. The individual forward solutions for current dipoles placed at these vertices comprised the columns of the gain matrix (**A**). A noise covariance matrix (**C**) was estimated from the raw MEG/EEG data during a 20–200-ms pre-stimulus baseline. These two matrices, along with the source covariance matrix **R**, were used to calculate the MNE inverse operator $\mathbf{W} = \mathbf{R}\mathbf{A}^{\mathrm{T}}(\mathbf{A}\mathbf{R}\mathbf{A}^{\mathrm{T}} + \mathbf{C})^{-1}$.

To obtain an fMRI prior, i.e., an fMRI-weighted source covariance matrix, each vertex point in the cortical surface was assigned an fMRI significance value using FreeSurfer-FSFAST 5.0. Individual functional volumes were motion corrected, unwarped, coregistered with each subject's structural MRI, intensity normalized, resampled into cortical surface space, smoothed using a 2-dimensional Gaussian kernel with an FWHM of 5 mm, and entered into a general-linear model (GLM) with the task conditions as explanatory variables. The fMRI weighting was set to 90%. That is, diagonal elements in **R** corresponding to vertices with below-threshold ($P < 0.01$, all conditions vs. baseline) significance values were multiplied by 0.1 (group fMRI result was used as a prior in 3 subjects). To investigate phase-locking between IPS and ACs, the entire MEG/EEG raw data time series at each time point were multiplied by the inverse operator **W** and noise normalized to yield the estimated source activity as a function of time within the right and left superior temporal cortices (Lin et al., 2006). In addition, the IPS seed regions were selected from each hemisphere using the Freesurfer anatomical atlas (Fischl et al., 2004). An average raw data time course was then calculated within these IPS seed regions, with the waveform signs of sources aligned on the basis of surface-normal orientations to avoid phase cancellations.

Accepted MEG/EEG/fMRI trial epochs were analyzed using the FieldTrip toolbox (http://www.ru.nl/fcdonders/fieldtrip) in Matlab 7.11 (Mathworks, Natick, MA). To investigate the phase locking between the IPS seed regions, a FFT taper approach with sliding time windows was applied on (**a**) the raw data epochs in each vertex of the right and left superior temporal cortex (as identified based on the Freesurfer atlas) and (**b**) on the corresponding trials of the pooled raw time courses of the right and left IPS, between −500 and 800 ms

relative to the sound onset, at 10-ms intervals. A priori, we hypothesized that the strongest inter-regional phase locking patterns would occur in theta and alpha, and lower beta ranges. Therefore, the FFT was applied at 3-Hz intervals at 4–19 Hz with an adaptive time-window of 3 cycles and a Hanning taper (i.e., the time window decreased from 750 to 158 ms as a function of the center frequency, respectively). The window length and taper were chosen based on previous studies (Osipova et al., 2006; Park et al., 2010). The 3-Hz intervals for TFR analyses were chosen because at 10 Hz, i.e., at the hypothesized center frequency of alpha oscillations, the frequency resolution of Hanning-window FFT is approximately 3 Hz. We then calculated the phase locking between the IPS seeds and each vertex of the superior temporal cortex patches using the pairwise phase consistency (PPC), weighted by the magnitude of the cross-spectrum. PPC is an estimator of the squared phase locking value (PLV) (for example, a PPC of 0.01 corresponds to PLV of 0.1) (Vinck et al., 2010). Unlike PLV, PPC is not biased by the number of available trials. The resulting PPC estimates between IPS and AC, mapped in each vertex of the AC patches, were then normalized to the Freesurfer standard brain representation (Fischl et al., 1999). To compare the cross hemispheric functional coupling patterns, we coregistered the two hemispheres into a common space in all subjects, using surface-based anatomical registration methods that align cortical folding patterns across both subject and hemisphere (Greve et al., 2013). Finally, in addition to the auditory-cortex mapping analysis, we calculated PPC between IPS and selected three regions-of-interest (ROI) from superior temporal ACs, including (**a**) Heschl's gyrus (HG; combined transverse temporal sulcus and gyrus, Destrieux et al. 2010), (**b**) the planum temporale (PT), (**c**) the posterior superior temporal gyrus (pSTG), and (**d**) the anterior STG (aSTG). These four AC ROIs were determined based on the Freesurfer atlas of (Destrieux et al., 2010), except for the borderline between pSTG and aSTG that was identified based on the FSL Harvard-Oxford cortical atlas structures “Superior Temporal Gyrus"Anterior Division" and "Superior Temporal Gyrus—Posterior Division" (http://fsl.fmrib.ox.ac.uk/fsl/fslwiki/Atlases) (Desikan et al., 2006).

2.4. Statistical analysis

All analyses reflect responses to attended non-target sounds, as analyzed from the AC contralateral to the attended ear. In other words, we calculated (**a**) PPC between the right vs. left IPS to left AC with the subjects attending the (contralateral) right ear and (**b**) between the right vs. left IPS and the right AC with the subjects attending to the left ear. As mentioned above, the parietotemporal PPC was compared in the common surface space (AC surface patch), co-registered based surface-based anatomical registration methods (Greve et al., 2013). In addition to direct comparisons of cross-hemispheric PPC patterns to test our main hypothesis (e.g., left IPS to right AC during attention to the left ear *vs*. right IPS and left AC during attention to the right ear), we conducted factorial analyses where the effect of hemisphere differences (e.g., due to distinct source cancellation patterns) was controlled.

Analyses of AC PPC maps were established using a nonparametric randomization test (Maris and Oostenveld, 2007). Vertices where the *t* statistics exceeded a critical value (two-tail $P < 0.05$) of a particular comparison were first identified, and clustered based on their adjacency in time, frequency, and across the (two-dimensional) cortical sheet (vertex-by-vertex connectivity matrix was determined by scripts from the Brainstorm package, http://neuroimage.usc.edu/brainstorm (Tadel et al., 2011)). The sum of *t* values within a cluster was used as cluster-level statistic, and the cluster with the maximum sum was used as test statistic in the non-parametric randomization procedure where the data was randomized across the two conditions and recalculated 10,000 times to obtain a reference distribution to evaluate the statistic of the actual data (Maris and Oostenveld, 2007).

In addition to the mapping analyses, we compared PPC between the IPS seed and the four AC subregions defined separately in each hemisphere. In the ROI analyses, the PPC values were pooled across 50–650 ms after attended non-target sound onsets. The ROI data were analyzed using non-parametric two-way Friedman ANOVA, with a priori comparisons of medians calculated using Wilcoxon ranked sum tests.

3. Results

3.1. Behavioral performance

The subjects' mean ± SD RT was 466 ± 100 ms and hit rates (HR) 90 ± 10% during MEG/EEG. During fMRI measurements, the mean ± SD RT was 495 ± 48 ms and the mean ± SD HR was 90 ± 8%. There was no significant difference between either behavioral measure obtained during the MEG/EEG and fMRI acquisitions.

3.2. Mapping of IPS phase locking across AC surface points

Our main hypothesis was that the left IPS has a more lateralized representation of acoustic space, limited to the right acoustic hemispace, while the right IPS was hypothesized to represent the acoustic space more bilaterally. This hypothesis was tested in two ways. First, in the AC region, we directly compared the maps representing PPC between the right IPS and left AC ($\boldsymbol{PPC}_{\mathbf{Right\ IPS\times Left\ AC}}$) during attention to the right ear *vs*. PPC between the left IPS and the right AC ($\boldsymbol{PPC}_{\mathbf{Left\ IPS\times Right\ AC}}$) during attention to the left ear. For this analysis, each subject's right and left AC was co-registered to a common surface representation using anatomical registration methods that align cortical folding patterns across both subject and hemisphere (Greve et al., 2013). As shown by the data in Figure 3, the $\boldsymbol{PPC}_{\mathbf{Left\ IPS\times Right\ AC}}$ during left-ear attention was significantly smaller than $\boldsymbol{PPC}_{\mathbf{Right\ IPS\times Left\ AC}}$ during right-ear attention, with the strongest differences peaking at 180 ms after sound onset. The differences were concentrated at 10–13 Hz, i.e., at the alpha range, but spanned also to the theta (7 Hz) and lower beta (16–19 Hz) frequencies. Anatomically, the differences in the phase locking between AC and the contralateral IPS concentrated in HG and the lateral aspects of non-primary AC (posterior superior temporal gyrus, pSTG; planum temporale, PT).

Recent studies have shown differences in the local cancellation patterns in MEG/EEG estimates across the left and right AC (Shaw et al., 2013). Therefore, to normalize out potential differences in source estimates across the left and right AC, we conducted an additional factorial analysis, where the intra- *vs*. cross-hemispheric effects were first normalized within each hemisphere (Figure 4). Consistent with our hypothesis (Figure 1), the difference between intra- vs. cross-hemispheric PPC between IPS and AC was significantly larger in the right hemisphere ($\boldsymbol{PPC}_{\mathbf{Right\ IPS\times Right\ AC}} - \boldsymbol{PPC}_{\mathbf{Left\ IPS\times Right\ AC}}$) during left-ear attention than in the left hemisphere ($\boldsymbol{PPC}_{\mathbf{Left\ IPS\times Left\ AC}} - \boldsymbol{PPC}_{\mathbf{Right\ IPS\times Left\ AC}}$) during right ear-attention at the boundary between alpha and theta ranges, i.e., at 7 Hz. In other words, the cross-hemispheric influence seemed to be weaker from the left IPS to the right AC than from the right IPS to the left AC, when the attention was focused to the ear contralateral of each AC. The significant PPC difference peaked at 340–380 ms after the sound onset, concentrating anatomically in HG, PT, and pSTG.

3.3. Phase locking between IPS and AC regions-of-interest

The results of our confirmatory ROI analyses, using two-way Friedman's ANOVA models to test the difference between ($\boldsymbol{PPC}_{\mathbf{Right\ IPS\times Right\ AC}} - \boldsymbol{PPC}_{\mathbf{Left\ IPS\times Right\ AC}}$) during left-ear attention *vs*. ($\boldsymbol{PPC}_{\mathbf{Left\ IPS\times Left\ AC}} - \boldsymbol{PPC}_{\mathbf{Right\ IPS\times Left\ AC}}$) during right-ear attention across all frequencies, were consistent with the above PPC mapping analyses. Specifically, as evaluated between 50–650 ms after stimulus, the difference between intra- vs. cross-

hemispheric PPC between IPS and AC was significantly larger in the right hemisphere during left-ear attention than that in the left hemisphere during right ear-attention, as analyzed in HG ($\chi^2 = 24.2$, $p < 0.001$) and PT ($\chi^2 = 6.6$, $p = 0.01$). That is, the left HG and PT seemed to be functionally coupled with both right and left IPS during right-ear attention, whereas the right HG and PT were significantly more strongly connected to the right than left IPS.

Table 1 shows the group median PPC values in the four different connections analyzed, between the IPS and ACs. The a priori comparisons of medians with Wilcoxon signed rank tests suggested that, during left-ear attention, the right HG was significantly more strongly phase locked with the right than left IPS at 4 Hz ($Z = -2.9$, $p < 0.01$), 7 Hz ($Z = -2.7$, $p < 0.01$), 10 Hz ($Z = -2.7$, $p < 0.01$), and 19 Hz ($Z = -2.8$, $p < 0.01$). Similar effect was observed in the right PT at 4 Hz ($Z = -2.1$, $p < 0.05$) and 10 Hz ($Z = -2.1$, $p < 0.05$) and in the right pSTG at 10 Hz ($Z = -1.96$, $p < 0.05$) and at 19 Hz ($Z = -2.2$, $p < 0.05$). There were also two instances of significant differences in the left AC during rightear attention. However, in both these cases, there was actually a stronger influence between the left AC and the cross-hemispheric, i.e., right IPS, as observed at 7 Hz in the left PT ($Z = -1.96$, $p < 0.05$) and pSTG ($Z = -2.1$, $p < 0.05$). Notably, the overall the intra-hemispheric parietotemporal PPC was not, however, weaker in the left hemisphere during right-ear attention than in the right hemisphere during left-ear attention.

4. Discussion

Here, we used combined MEG/EEG/fMRI to compare oscillatory phase locking, quantified as PPC, between AC and IPS during auditory spatial selective attention. Our results suggest asymmetric attentional PPC modulations, supporting the hypothesis that the right IPS might have a more global bilateral representation of acoustic space than the left IPS. That is, PPC was stronger between the right IPS and left AC than between the left IPS and right AC, when attention was in each condition directed to the ear contralateral to the AC of interest. In the cortical mapping analyses, the differences in PPC between IPS and AC were most predominant in the theta and alpha ranges, between 7–13 Hz. In the ROI analyses, significant differences were also found in the lower theta (4 Hz) and lower beta ranges (19 Hz).

Our results are in line with previous studies supporting the "neglect model", positing that the right parietal cortex controls attention to both hemifields and that the left posterior parietal cortex has a representation only for the contralateral right hemifield in healthy human subjects (At et al., 2011; Spierer et al., 2009; Tanaka et al., 1999; Teshiba et al., 2012). As estimated from the direct comparison between $\boldsymbol{PPC}_{\textbf{Left IPS×Right AC}}$ during left-ear attention and $\boldsymbol{PPC}_{\textbf{Right IPS×Left AC}}$ during right-ear attention, significant differences occurred at early stages of stimulus processing, peaking already at 180 ms after sound onset at the alpha frequencies. Although the time resolution of sliding-window phase-locking analyzes is limited, it is interesting to note that recent TMS studies have suggested temporally distinct modulations of auditory spatial processing performance, with TMS manipulations delivered to the right parietal cortex at 80 ms after sound onsets resulting in a generalized localization deficit (At et al., 2011). In other words, the time window of these TMS manipulations would have been roughly suitable for interrupting the evolution of the most clearly lateralized PPC pattern between IPS and AC.

Here, the functional coupling between IPS and AC during auditory attention was measured by analyzing long-range phase locking of neuronal oscillations. Our analysis concentrated on oscillatory phase locking at the 4–19 Hz range, encompassing the theta, alpha, and lower beta bands, which are presumed to be particularly suitable for longer-range functional

coupling of distant oscillatory neuron populations (Engel et al., 2001; Ermentrout and Kopell, 1998; Kopell et al., 2000; von Stein and Sarnthein, 2000), in contrast to higher-frequency gamma oscillations being most clearly associated with enhancing local processing of task-relevant features (Buschman and Miller, 2007; Varela et al., 2001). Indeed, while the present spatio-spectrotemporal clusters of significant effects extended at up to 19 Hz, the major patterns associated with lateralized functional connectivity patterns between IPS and AC occurred at the theta and alpha ranges. This observation is concert with previous studies suggesting long-range theta (Harris et al., 2002; Jensen, 2001; Moore et al., 2006) and alpha (Palva and Palva, 2007; Schack et al., 2005) phase coupling is associated with attention and working memory. For example, a recent study has found that alpha-band phase coupling between frontoparietal brain regions (Palva et al., 2010) predicts individual WM capacity, and is consistent with the idea that alpha may underlie suppression of irrelevant information and selection or sharpening of relevant information (Hanslmayr et al., 2011; Klimesch, 2012). Further, there is evidence that during visual tasks, alpha phase and high gamma amplitude coupling preferentially increases in visual cortical regions (Voytek et al., 2010).

If low-frequency oscillatory phenomena indeed reflect the neuronal mechanisms underlying selective attention and cortico-cortical communication (Hanslmayr et al., 2011), one might expect right hemisphere dominance of low-frequency oscillations in the auditory attention network. The present findings, suggesting a more bilateral alpha-range PPC between right than left IPS and auditory areas during selective attention, are clearly consistent with this notion. Evidence for such lateralization pattern was also found in a recent study (Müller and Weisz, 2012) that suggested asymmetric modulation of auditory alpha power following external cues with right hemisphere dominance. The present results are also consistent with another recent auditory functional connectivity study (Weisz et al., 2013) that showed significantly increased effective connectivity between the right IPS and AC during cued auditory spatial attention, as measures with alpha-range PDC.

In addition to the phase locking differences concentrated at the low frequency ranges including theta and alpha, our data also indicate that the differences span to lower beta-band (16–19 Hz). Several studies have suggested a role for large-scale coupling in the beta-band associated with sensorimotor integration (for review, see Siegel et al., 2012) and top-down influences in other cognitive domains (Engel and Fries, 2010; Keil et al., 2013). A recent animal study using a sustained attention task demonstrated that anterior cingulate cortex neurons are phase locked to the prelimbic beta oscillations exclusively on correct trials, and while on incorrect trials, there were no phase locked neurons (Totah et al., 2012). Human MEG studies have also shown frontoparietal beta-band activity associated with perceptual decision-making processes (Donner et al., 2007). Taken together, our finding is consistent with the above evidence and the idea that large scale oscillations in a lower beta-band (12–25 Hz) may play a role in connecting the sensory and motor processing stages of the decision process (Donner et al., 2007).

The present design was constrained to one higher order parietal region per hemisphere, namely IPS, based on recent studies indicating the crucial role of this region in spatial attention (Vandenberghe and Gillebert, 2009), both in the auditory (Cohen et al., 2005; Huang et al., 2012; Kong et al., 2012; Weisz et al., 2013) and visual domains (Greenberg et al., 2012; Silver and Kastner, 2009). Anatomically, IPS may be human homologue of the lateral intra parietal (LIP) area in nonhuman primates (Vandenberghe and Gillebert, 2009), which has been postulated to be involved in the compilation of an attentional priority map, a topographic representation of the distribution of attentional weights (Ptak, 2012; Vandenberghe et al., 2012). Importantly, neurophysiological studies have shown that the monkey homologue of human IPS contains modality-specific neurons activated selectively during auditory attention tasks (Cohen et al., 2005). Although the most significant

activations have typically been described in the right IPS (Weisz et al., 2013), several recent studies have also described bilateral IPS activations during voluntary auditory spatial attention (Huang et al., 2012; Kong et al., 2012; Salmi et al., 2009). The choice of IPS was also supported by the feasibility of selecting this seed region based on purely independent anatomical criteria (Destrieux et al., 2010), as implemented in the Freesurfer surface based cortical parcellation (Fischl et al., 2004). In contrast, other regions that might have been quite interesting, such as the FEF, cannot be delineated based on equally clear anatomical atlas criteria.

Our ROI analyses suggested strongest lateralization patterns of parietotemporal PPC in HG. This might be somewhat surprising, given that auditory attention studies, generally, suggest strongest attentional top-down modulations in more lateral non-primary areas of AC. However, it is noteworthy that recent fMRI studies in humans have also suggested that the contra-lateralization of responses to monaural sounds is strongest in the putative core areas of AC, while the more lateral aspects of non-primary ACs represent more bilateral response patterns (Langers et al., 2007; Woods et al., 2009).

Notably, the time resolution of oscillatory analyses is inherently limited. Analogously to many previous studies (Osipova et al., 2006; Park et al., 2010), we used an adaptive time window of three cycles / frequency in the oscillatory analyses, resulting in a 750-ms sliding window at the lowest 4-Hz center frequency and a 157 ms window at the highest 19-Hz frequency. For example, at 4 Hz, the values reported at each time point are, thus, weighted averages of activities within 375 ms before and after the center point of the analysis window. However, because the sliding window is tapered, the estimate of the instantaneous phase is strongly weighted towards the midpoint of the window. A related notion is that, particularly at the higher frequencies, there may be overlap across the adjacent frequency bins. In the present study, we have considered the effects observed at 7 Hz to reflect the theta band. With the present settings, the bandwidth of the analysis is 5.8–8.2 Hz with the 7-Hz center frequency. Consequently, the effects could be interpreted to involve some influence from the lower alpha band as well. Finally, it should also be noted that, because of the adaptive time window, the estimates are more smooth over time at the lower frequencies and more smooth over the frequency axis at higher frequencies (as the spectral bandwidth of the Hanning window FFT is the inverse of the window length). Consequently, the PPC values will correlate more over time at lower frequencies and more over the frequency at higher frequencies. This might increase the probability of finding clusters continuous over the time axis at lower frequencies and those continuous over the frequency at higher frequencies. Nevertheless, the adaptive windowing, which has been utilized in numerous previous studies applying wavelet transforms to determine instantaneous phase or power values, could be assumed to be a less biased approach than using a fixed window. With a long fixed time window, the brief synchronization patterns at higher frequencies could remain undetected and the results would be inherently biased toward the lower frequencies.

5. Conclusions

To sum up, our data is consistent of the “neglect model” suggesting that the right parietal cortex has a bilateral representation of space, whereas the left parietal cortex has a more limited right-lateralized space representation. The parietotemporal functional connectivity patterns underlying selective auditory spatial attention may be dominated by alpha-range oscillations.

Acknowledgments

We thank An-Yi Hung, Natsuko Mori, Stephanie Rossi, Chinmayi Tengshe, and Nao Suzuki for their help. This work was supported by National Institutes of Health Awards R01MH083744, R21DC010060, R01HD040712, R01NS037462, and 5R01EB009048. This research was carried out at the Athinoula A. Martinos Center for Biomedical Imaging at the Massachusetts General Hospital, using resources provided by the Center for Functional Neuroimaging Technologies, P41EB015896, a P41 Biotechnology Resource Grant supported by the National Institute of Biomedical Imaging and Bioengineering (NIBIB), National Institutes of Health. The research environment was additionally supported by National Center for Research Resources Shared Instrumentation Grants S10RR014978, S10RR021110, S10RR019307, S10RR014798, and S10RR023401.

References

Ahveninen J, Hamalainen M, Jaaskelainen IP, Ahlfors SP, Huang S, Lin FH, Raij T, Sams M, Vasios CE, Belliveau JW. Attention-driven auditory cortex short-term plasticity helps segregate relevant sounds from noise. Proc Natl Acad Sci U S A. 2011; 108:4182–4187. [PubMed: 21368107]

Ahveninen J, Huang S, Belliveau JW, Chang WT, Hämäläinen M. Dynamic oscillatory processes governing cued orienting and allocation of auditory attention. J Cogn Neurosci. 2013; 25:1926–1943. [PubMed: 23915050]

Ahveninen J, Jaaskelainen IP, Belliveau JW, Hamalainen M, Lin FH, Raij T. Dissociable influences of auditory object vs. spatial attention on visual system oscillatory activity. PLoS One. 2012; 7:e38511. [PubMed: 22693642]

Ahveninen J, Jaaskelainen IP, Raij T, Bonmassar G, Devore S, Hamalainen M, Levanen S, Lin FH, Sams M, Shinn-Cunningham BG, Witzel T, Belliveau JW. Task-modulated "what" and "where" pathways in human auditory cortex. Proc Natl Acad Sci U S A. 2006; 103:14608–14613. [PubMed: 16983092]

Alho K, Medvedev SV, Pakhomov SV, Roudas MS, Tervaniemi M, Reinikainen K, Zeffiro T, Näätänen R. Selective tuning of the left and right auditory cortices during spatially directed attention. Brain Research. Cognitive Brain Research. 1999; 7:335–341. [PubMed: 9838184]

Alho K, Vorobyev VA, Medvedev SV, Pakhomov SV, Roudas MS, Tervaniemi M, van Zuijen T, Näätänen R. Hemispheric lateralization of cerebral blood-flow changes during selective listening to dichotically presented continuous speech. Brain Res Cogn Brain Res. 2003; 17:201–211. [PubMed: 12880891]

At A, Spierer L, Clarke S. The role of the right parietal cortex in sound localization: a chronometric single pulse transcranial magnetic stimulation study. Neuropsychologia. 2011; 49:2794–2797. [PubMed: 21679720]

Baumgart F, Gaschler-Markefski B, Woldorff MG, Heinze HJ, Scheich H. A movement-sensitive area in auditory cortex. Nature. 1999; 400:724–726. [PubMed: 10466721]

Bisiach E, Cornacchia L, Sterzi R, Vallar G. Disorders of perceived auditory lateralization after lesions of the right hemisphere. Brain. 1984; 107(Pt 1):37–52. [PubMed: 6697161]

Buschman TJ, Miller EK. Top-down versus bottom-up control of attention in the prefrontal and posterior parietal cortices. Science. 2007; 315:1860–1862. [PubMed: 17395832]

Cohen YE, Russ BE, Gifford GW 3rd. Auditory processing in the posterior parietal cortex. Behav Cogn Neurosci Rev. 2005; 4:218–231. [PubMed: 16510894]

Dale AM, Liu AK, Fischl BR, Buckner RL, Belliveau JW, Lewine JD, Halgren E. Dynamic statistical parametric mapping: combining fMRI and MEG for high-resolution imaging of cortical activity. Neuron. 2000; 26:55–67. [PubMed: 10798392]

Desikan R, Segonne F, Fischl B, Quinn B, Dickerson B, Blacker D, Buckner R, Dale A, Maguire R, Hyman B, Albert M, Killiany R. An automated labeling system for subdividing the human cerebral cortex on MRI scans into gyral based regions of interest. Neuroimage. 2006; 31:968–980. [PubMed: 16530430]

Destrieux C, Fischl B, Dale A, Halgren E. Automatic parcellation of human cortical gyri and sulci using standard anatomical nomenclature. Neuroimage. 2010; 53:1–15. [PubMed: 20547229]

Donner TH, Siegel M, Oostenveld R, Fries P, Bauer M, Engel AK. Population activity in the human dorsal pathway predicts the accuracy of visual motion detection. J Neurophysiol. 2007; 98:345–359. [PubMed: 17493916]

Engel AK, Fries P. Beta-band oscillations — signalling the status quo? Curr Opin Neurobiol. 2010; 20:156–165. [PubMed: 20359884]

Engel AK, Fries P, Singer W. Dynamic predictions: oscillations and synchrony in top-down processing. Nat Rev Neurosci. 2001; 2:704–716. [PubMed: 11584308]

Ermentrout GB, Kopell N. Fine structure of neural spiking and synchronization in the presence of conduction delays. Proc Natl Acad Sci U S A. 1998; 95:1259–1264. [PubMed: 9448319]

Fischl B, Sereno MI, Tootell RB, Dale AM. High-resolution intersubject averaging and a coordinate system for the cortical surface. Hum Brain Mapp. 1999; 8:272–284. [PubMed: 10619420]

Fischl B, van der Kouwe A, Destrieux C, Halgren E, Segonne F, Salat DH, Busa E, Seidman LJ, Goldstein J, Kennedy D, Caviness V, Makris N, Rosen B, Dale AM. Automatically parcellating the human cerebral cortex. Cereb Cortex. 2004; 14:11–22. [PubMed: 14654453]

Grady CL, Van Meter JW, Maisog JM, Pietrini P, Krasuski J, Rauschecker JP. Attention-related modulation of activity in primary and secondary auditory cortex. Neuroreport. 1997; 8:2511–2516. [PubMed: 9261818]

Greenberg AS, Verstynen T, Chiu YC, Yantis S, Schneider W, Behrmann M. Visuotopic cortical connectivity underlying attention revealed with white-matter tractography. J Neurosci. 2012; 32:2773–2782. [PubMed: 22357860]

Greve DN, Van der Haegen L, Cai Q, Stufflebeam S, Sabuncu MR, Fischl B, Brysbaert M. A Surface-based Analysis of Language Lateralization and Cortical Asymmetry. J Cogn Neurosci. 2013; 25:1477–1492. [PubMed: 23701459]

Griffiths TD, Rees G, Rees A, Green GG, Witton C, Rowe D, Buchel C, Turner R, Frackowiak RS. Right parietal cortex is involved in the perception of sound movement in humans. Nat Neurosci. 1998; 1:74–79. [PubMed: 10195113]

Gross J, Schmitz F, Schnitzler I, Kessler K, Shapiro K, Hommel B, Schnitzler A. Modulation of long-range neural synchrony reflects temporal limitations of visual attention in humans. Proc Natl Acad Sci U S A. 2004; 101:13050–13055. [PubMed: 15328408]

Hämäläinen M, Hari R, Ilmoniemi R, Knuutila J, Lounasmaa O. Magnetoencephalography - theory, instrumentation, and applications to noninvasive studies of the working human brain. Rev. Mod. Phys. 1993; 65:413–497.

Hansen JC, Hillyard SA. Endogenous brain potentials associated with selective auditory attention. Electroencephalography & Clinical Neurophysiology. 1980; 49:277–290. [PubMed: 6158404]

Hanslmayr S, Gross J, Klimesch W, Shapiro KL. The role of alpha oscillations in temporal attention. Brain Res Rev. 2011; 67:331–343. [PubMed: 21592583]

Harris K, Henze D, Hirase H, Leinekugel X, Dragoi G, Czurko A, Buzsaki G. Spike train dynamics predicts theta-related phase precession in hippocampal pyramidal cells. Nature. 2002; 417:738–741. [PubMed: 12066184]

Hart HC, Palmer AR, Hall DA. Different areas of human non-primary auditory cortex are activated by sounds with spatial and nonspatial properties. Hum Brain Mapp. 2004; 21:178–190. [PubMed: 14755837]

Hillyard S, Hink R, Schwent V, Picton T. Electrical signs of selective attention in the human brain. Science. 1973; 182:177–180. [PubMed: 4730062]

Huang S, Belliveau JW, Tengshe C, Ahveninen J. Brain networks of novelty-driven involuntary and cued voluntary auditory attention shifting. PLoS ONE. 2012; 7:e44062. [PubMed: 22937153]

Jenkins WM, Masterton RB. Sound localization: effects of unilateral lesions in central auditory system. J Neurophysiol. 1982; 47:987–1016. [PubMed: 7108581]

Jensen O. Information transfer between rhythmically coupled networks: reading the hippocampal phase codex. Neural Comput. 2001 Dec; 13(12):2743–2761. Neural Computing 13, 2743–2761. [PubMed: 11705409]

Jensen O, Kaiser J, Lachaux JP. Human gamma-frequency oscillations associated with attention and memory. Trends Neurosci. 2007; 30:317–324. [PubMed: 17499860]

Kaiser J, Lutzenberger W, Preissl H, Ackermann H, Birbaumer N. Right-hemisphere dominance for the processing of sound-source lateralization. Journal of Neuroscience. 2000; 20:6631–6639. [PubMed: 10964968]

Keil J, Muller N, Hartmann T, Weisz N. Prestimulus Beta Power and Phase Synchrony Influence the Sound-Induced Flash Illusion. Cereb Cortex. 2013

Klimesch W. alpha-band oscillations, attention, and controlled access to stored information. Trends Cogn Sci. 2012; 16:606–617. [PubMed: 23141428]

Kong L, Michalka SW, Rosen ML, Sheremata SL, Swisher JD, Shinn-Cunningham BG, Somers DC. Auditory Spatial Attention Representations in the Human Cerebral Cortex. Cereb Cortex. 2012

Kopell N, Ermentrout GB, Whittington MA, Traub RD. Gamma rhythms and beta rhythms have different synchronization properties. Proc Natl Acad Sci U S A. 2000; 97:1867–1872. [PubMed: 10677548]

Krumbholz K, Schonwiesner M, von Cramon DY, Rubsamen R, Shah NJ, Zilles K, Fink GR. Representation of interaural temporal information from left and right auditory space in the human planum temporale and inferior parietal lobe. Cereb Cortex. 2005; 15:317–324. [PubMed: 15297367]

Langers DR, Backes WH, van Dijk P. Representation of lateralization and tonotopy in primary versus secondary human auditory cortex. Neuroimage. 2007; 34:264–273. [PubMed: 17049275]

Lin FH, Belliveau JW, Dale AM, Hämäläinen MS. Distributed current estimates using cortical orientation constraints. Hum Brain Mapp. 2006; 27:1–13. [PubMed: 16082624]

Lin FH, Witzel T, Hämäläinen MS, Dale AM, Belliveau JW, Stufflebeam SM. Spectral spatiotemporal imaging of cortical oscillations and interactions in the human brain. Neuroimage. 2004; 23:582–595. [PubMed: 15488408]

Maris E, Oostenveld R. Nonparametric statistical testing of EEG- and MEG-data. J Neurosci Methods. 2007; 164:177–190. [PubMed: 17517438]

Mayer AR, Franco AR, Harrington DL. Neuronal modulation of auditory attention by informative and uninformative spatial cues. Hum Brain Mapp. 2009; 30:1652–1666. [PubMed: 18661505]

Mayer AR, Harrington D, Adair JC, Lee R. The neural networks underlying endogenous auditory covert orienting and reorienting. Neuroimage. 2006; 30:938–949. [PubMed: 16388970]

Moore RA, Gale A, Morris PH, Forrester D. Theta phase locking across the neocortex reflects cortico-hippocampal recursive communication during goal conflict resolution. Int J Psychophysiol. 2006; 60:260–273. [PubMed: 16168505]

Müller N, Weisz N. Lateralized auditory cortical alpha band activity and interregional connectivity pattern reflect anticipation of target sounds. Cereb Cortex. 2012; 22:1604–1613. [PubMed: 21893682]

Osipova D, Takashima A, Oostenveld R, Fernandez G, Maris E, Jensen O. Theta and gamma oscillations predict encoding and retrieval of declarative memory. J Neurosci. 2006; 26:7523–7531. [PubMed: 16837600]

Palomäki KJ, Tiitinen H, Mäkinen V, May PJ, Alku P. Spatial processing in human auditory cortex: the effects of 3D, ITD, and ILD stimulation techniques. Brain Res Cogn Brain Res. 2005; 24:364–379. [PubMed: 16099350]

Palva JM, Monto S, Kulashekhar S, Palva S. Neuronal synchrony reveals working memory networks and predicts individual memory capacity. Proc Natl Acad Sci U S A. 2010; 107:7580–7585. [PubMed: 20368447]

Palva S, Palva JM. New vistas for alpha-frequency band oscillations. Trends Neurosci. 2007; 30:150–158. [PubMed: 17307258]

Park HD, Min BK, Lee KM. EEG oscillations reflect visual short-term memory processes for the change detection in human faces. Neuroimage. 2010; 53:629–637. [PubMed: 20600967]

Petkov CI, Kang X, Alho K, Bertrand O, Yund EW, Woods DL. Attentional modulation of human auditory cortex. Nat Neurosci. 2004; 7:658–663. [PubMed: 15156150]

Ptak R. The frontoparietal attention network of the human brain: action, saliency, and a priority map of the environment. Neuroscientist. 2012; 18:502–515. [PubMed: 21636849]

Roelfsema PR, Engel AK, König P, Singer W. Visuomotor integration is associated with zero time-lag synchronization among cortical areas. Nature. 1997; 385:157–161. [PubMed: 8990118]

Ruff RM, Hersh NA, Pribram KH. Auditory spatial deficits in the personal and extrapersonal frames of reference due to cortical lesions. Neuropsychologia. 1981; 19:435–443. [PubMed: 7266836]

Salmi J, Rinne T, Koistinen S, Salonen O, Alho K. Brain networks of bottom-up triggered and top-down controlled shifting of auditory attention. Brain Res. 2009; 1286:155–164. [PubMed: 19577551]

Salminen NH, Tiitinen H, Miettinen I, Alku P, May PJ. Asymmetrical representation of auditory space in human cortex. Brain Res. 2010; 1306:93–99. [PubMed: 19799877]

Sanchez-Longo LP, Forster FM. Clinical significance of impairment of sound localization. Neurology. 1958; 8:119–125. [PubMed: 13504429]

Santangelo V, Olivetti Belardinelli M, Spence C, Macaluso E. Interactions between voluntary and stimulus-driven spatial attention mechanisms across sensory modalities. J Cogn Neurosci. 2009; 21:2384–2397. [PubMed: 19199406]

Sauseng P, Hoppe J, Klimesch W, Gerloff C, Hummel FC. Dissociation of sustained attention from central executive functions: local activity and interregional connectivity in the theta range. Eur J Neurosci. 2007; 25:587–593. [PubMed: 17284201]

Schack B, Klimesch W, Sauseng P. Phase synchronization between theta and upper alpha oscillations in a working memory task. Int J Psychophysiol. 2005; 57:105–114. [PubMed: 15949859]

Shaw ME, Hamalainen MS, Gutschalk A. How anatomical asymmetry of human auditory cortex can lead to a rightward bias in auditory evoked fields. Neuroimage. 2013; 74:22–29. [PubMed: 23415949]

Shomstein S, Yantis S. Control of attention shifts between vision and audition in human cortex. J Neurosci. 2004; 24:10702–10706. [PubMed: 15564587]

Shomstein S, Yantis S. Parietal cortex mediates voluntary control of spatial and nonspatial auditory attention. J Neurosci. 2006; 26:435–439. [PubMed: 16407540]

Siegel M, Donner TH, Engel AK. Spectral fingerprints of large-scale neuronal interactions. Nat Rev Neurosci. 2012; 13:121–134. [PubMed: 22233726]

Silver MA, Kastner S. Topographic maps in human frontal and parietal cortex. Trends Cogn Sci. 2009; 13:488–495. [PubMed: 19758835]

Singer W. Neuronal synchrony: a versatile code for the definition of relations? Neuron. 1999; 24:49–65. 111–125. [PubMed: 10677026]

Spierer L, Bellmann-Thiran A, Maeder P, Murray MM, Clarke S. Hemispheric competence for auditory spatial representation. Brain. 2009; 132:1953–1966. [PubMed: 19477962]

Tadel F, Baillet S, Mosher JC, Pantazis D, Leahy RM. Brainstorm: a user-friendly application for MEG/EEG analysis. Comput Intell Neurosci. 2011; 2011:879716. [PubMed: 21584256]

Tanaka H, Hachisuka K, Ogata H. Sound lateralisation in patients with left or right cerebral hemispheric lesions: relation with unilateral visuospatial neglect. J Neurol Neurosurg Psychiatry. 1999; 67:481–486. [PubMed: 10486395]

Taulu S, Simola J, Kajola M. Applications of the Signal Space Separation Method. IEEE Trans. Signal Proc. 2005; 53:3359–3372.

Teshiba TM, Ling J, Ruhl DA, Bedrick BS, Pena A, Mayer AR. Evoked and Intrinsic Asymmetries during Auditory Attention: Implications for the Contralateral and Neglect Models of Functioning. Cereb Cortex. 2012; 23:560–569. [PubMed: 22371310]

Tiitinen H, Salminen NH, Palomaki KJ, Makinen VT, Alku P, May PJ. Neuromagnetic recordings reveal the temporal dynamics of auditory spatial processing in the human cortex. Neurosci Lett. 2006; 396:17–22. [PubMed: 16343772]

Totah NK, Jackson ME, Moghaddam B. Preparatory Attention Relies on Dynamic Interactions between Prelimbic Cortex and Anterior Cingulate Cortex. Cereb Cortex. 2013; 23:729–738. [PubMed: 22419680]

Vandenberghe R, Gillebert CR. Parcellation of parietal cortex: Convergence between lesion-symptom mapping and mapping of the intact functioning brain. Behavioural Brain Research. 2009; 199:171–182. [PubMed: 19118580]

Vandenberghe R, Molenberghs P, Gillebert CR. Spatial attention deficits in humans: the critical role of superior compared to inferior parietal lesions. Neuropsychologia. 2012; 50:1092–1103. [PubMed: 22266260]

Varela F, Lachaux JP, Rodriguez E, Martinerie J. The brainweb: phase synchronization and large-scale integration. Nat Rev Neurosci. 2001; 2:229–239. [PubMed: 11283746]

Vinck M, van Wingerden M, Womelsdorf T, Fries P, Pennartz CM. The pairwise phase consistency: a bias-free measure of rhythmic neuronal synchronization. Neuroimage. 2010; 51:112–122. [PubMed: 20114076]

Virtanen J, Ahveninen J, Ilmoniemi RJ, Näätänen R, Pekkonen E. Replicability of MEG and EEG measures of the auditory N1/N1m-response. Electroencephalography & Clinical Neurophysiology. 1998; 108:291–298. [PubMed: 9607518]

von Stein A, Chiang C, König P. Top-down processing mediated by interareal synchronization. Proc Natl Acad Sci U S A. 2000; 97:14748–14753. [PubMed: 11121074]

von Stein A, Sarnthein J. Different frequencies for different scales of cortical integration: from local gamma to long range alpha/theta synchronization. International Journal of Psychophysiology. 2000; 38:301–313. [PubMed: 11102669]

Voytek B, Canolty RT, Shestyuk A, Crone NE, Parvizi J, Knight RT. Shifts in gamma phase-amplitude coupling frequency from theta to alpha over posterior cortex during visual tasks. Front Hum Neurosci. 2010; 4:191. [PubMed: 21060716]

Weisz N, Muller N, Jatzev S, Bertrand O. Oscillatory Alpha Modulations in Right Auditory Regions Reflect the Validity of Acoustic Cues in an Auditory Spatial Attention Task. Cereb Cortex. 2013

Woldorff MG, Hillyard SA, Gallen CC, Hampson SR, Bloom FE. Magnetoencephalographic recordings demonstrate attentional modulation of mismatch-related neural activity in human auditory cortex. Psychophysiology. 1998; 35:283–292. [PubMed: 9564748]

Womelsdorf T, Fries P. The role of neuronal synchronization in selective attention. Curr Opin Neurobiol. 2007; 17:154–160. [PubMed: 17306527]

Woods DL, Stecker GC, Rinne T, Herron TJ, Cate AD, Yund EW, Liao I, Kang X. Functional maps of human auditory cortex: effects of acoustic features and attention. PLoS ONE. 2009; 4:e5183. [PubMed: 19365552]

Wu CT, Weissman DH, Roberts KC, Woldorff MG. The neural circuitry underlying the executive control of auditory spatial attention. Brain Res. 2007; 1134:187–198. [PubMed: 17204249]

Zatorre RJ, Mondor TA, Evans AC. Auditory attention to space and frequency activates similar cerebral systems. Neuroimage. 1999; 10:544–554. [PubMed: 10547331]

Zatorre RJ, Penhune VB. Spatial localization after excision of human auditory cortex. J Neurosci. 2001; 21:6321–6328. [PubMed: 11487655]

Highlights

- Neuronal oscillations measured with MEG/EEG/fMRI during dichotic auditory attention
- Cross-hemispheric phase locking between auditory and parietal cortices analyzed
- Broader auditory spatial representation in the right than left parietal cortex
- Parietotemporal attentional coupling dominated by alpha-range oscillations

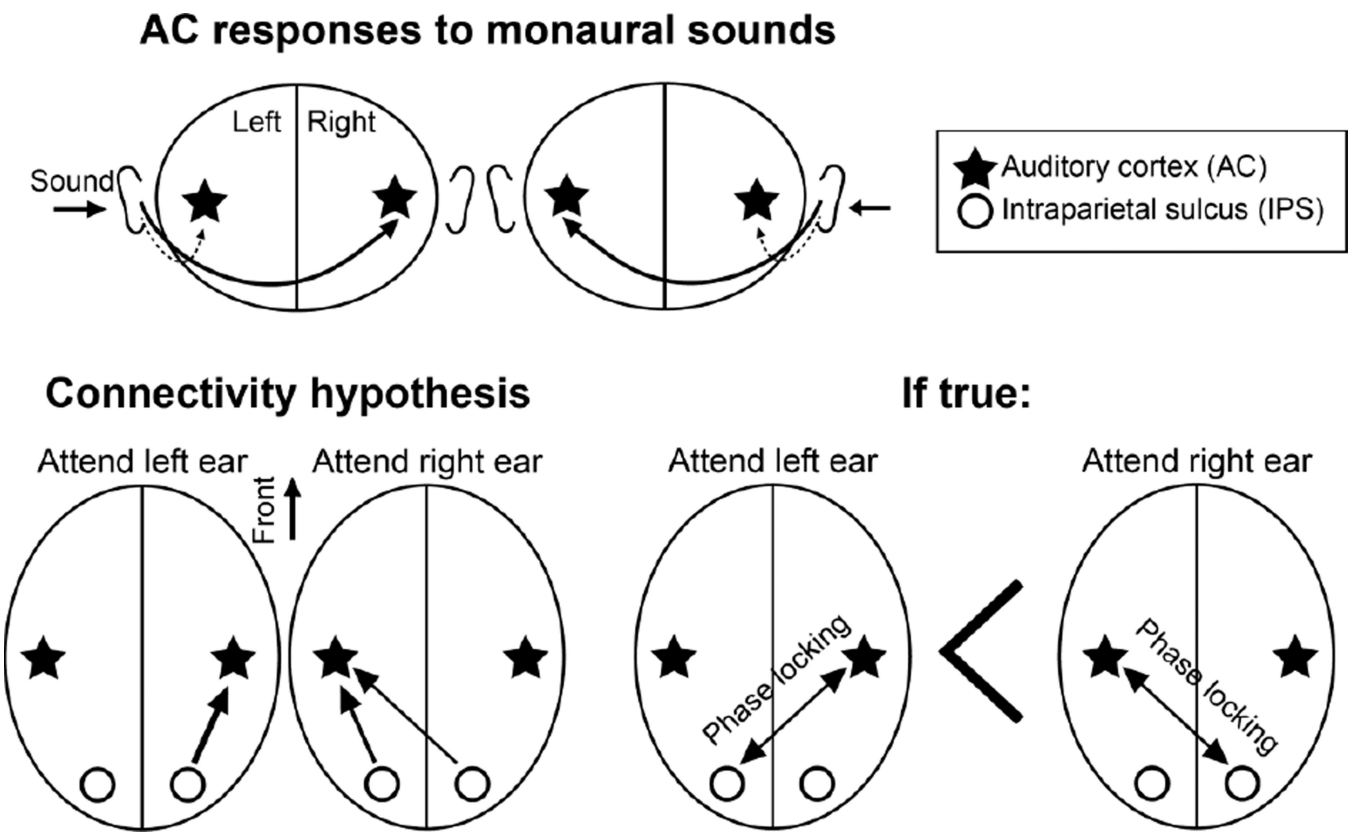

Figure 1.

Connectivity hypotheses. (**Top**) During dichotic listening, sound responses are presumed to be largest in the AC contralateral to the ear stimulated, although the ipsilateral AC will be stimulated as well. We therefore used contralateral AC responses for tagging the connectivity patterns during lateralized auditory attention. (**Bottom, Left**) Hypothesis of feedback modulations of lateralized AC responses by the left vs. right IPS during dichotic attention task. (**Bottom, Right**) If the presumed "neglect model" holds true, phase locking between the left IPS and right AC during left-ear attention should be weaker than phase locking between the right IPS and left AC during right-ear attention.

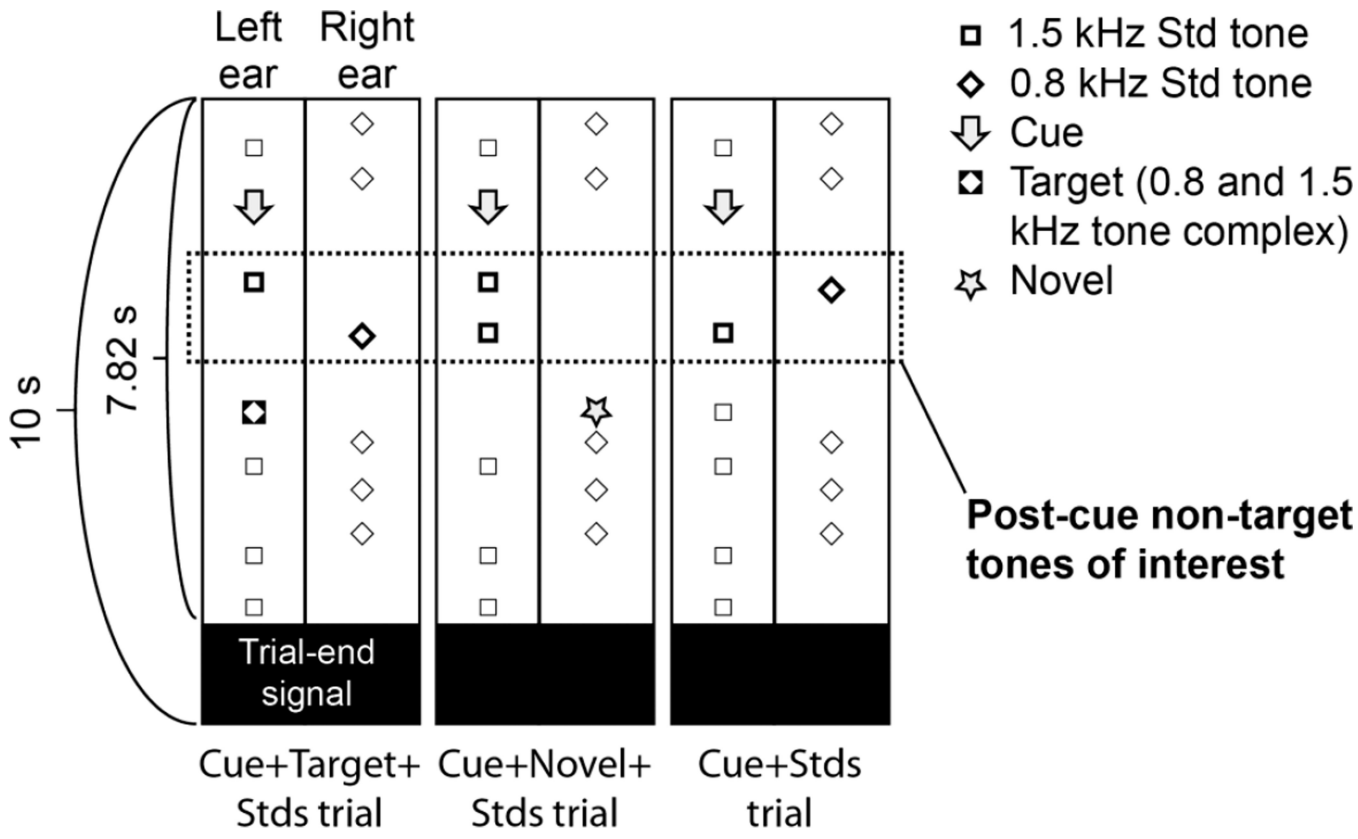

Figure 2.

Task design. At the onset of each trial, subjects started hearing standard sounds randomly in each ear (800-Hz pure tones in the right ear and 1500-Hz pure tones in the left ear). Subjects were instructed to shift and engage attention based on a monaural buzzer cue, and to discriminate a subsequent target stimulus (monaural 50-ms tone with 800- and 1500-Hz harmonics) that was embedded within the standard-sound sequence in the designated ear. The present analyses concentrated on phase locking patterns emerging after the two first tones (encircled) presented after these attention-shifting cues and before the subsequent "probes". The "probe" sound was the target in 40% of trials (Cue+Target+Stds trial), a task-irrelevant novel sound opposite to the cued ear in 20% of trials (Cue+Novel+Stds trial), or a standard sound replacing the target in 20% of trials (Cue+Stds trial). However, the attentional engagement preceding the probes was presumed to be similar across these trials, because the subjects were not informed of the trial type in advance. The remaining 20% of the trials, consisting of only standard sounds, were not analyzed.

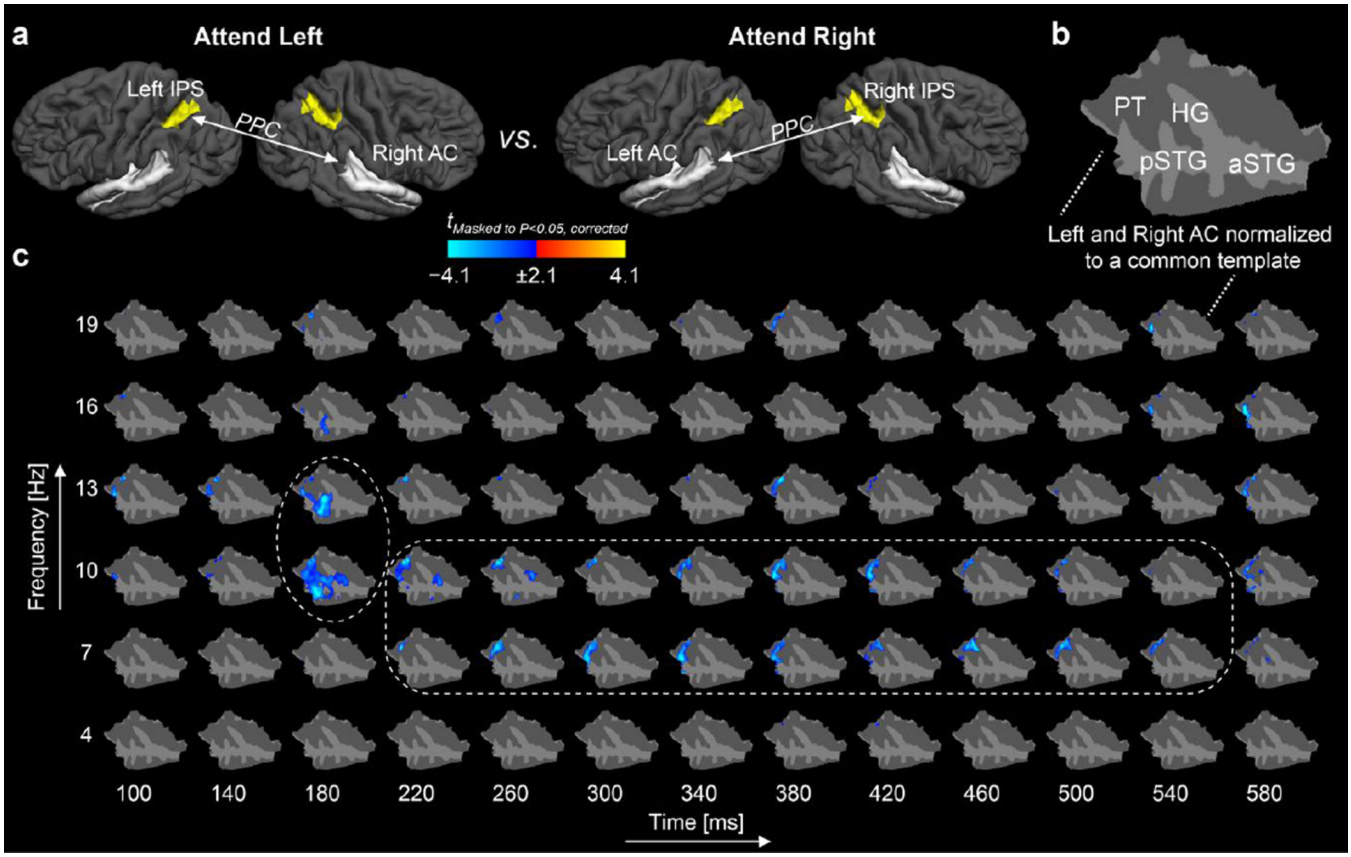

Figure 3.

Cross-hemispheric phase locking between IPS seeds and AC vertex points during dichotic auditory attention. (**a**) A schematic illustration of the PPC comparisons. (**b**) The left and right AC were co-registered to a common cortical surface template. (**c**) Spatial TFR of evolution of PPC differences between IPS and all vertices of AC after attended post-cue non-target tones (t = 0 ms refers to the tone onset). The statistic parametric map shows that the left IPS and right AC are more weakly synchronized than the right IPS and left AC, when attention is directed to the ear contralateral to each AC. The significant differences concentrated at 10–13 Hz, i.e., at the alpha range, but spanned also to the theta (7 Hz) and lower beta (16–19 Hz) frequencies (encircled). Taken together, these data support our hypothesis that the right parietal cortex has a more global representation of the acoustic space, spanning both the contralateral and ipsilateral hemifields, than the left parietal cortex. The figure shows t values masked to locations where the PPC differences were statistically significant (P<0.05, cluster-based randomization test). Abbreviations: HG, Heschl's gyrus; PT, planum temporale; pSTG, posterior superior temporal gyrus; aSTG anterior superior temporal gyrus.

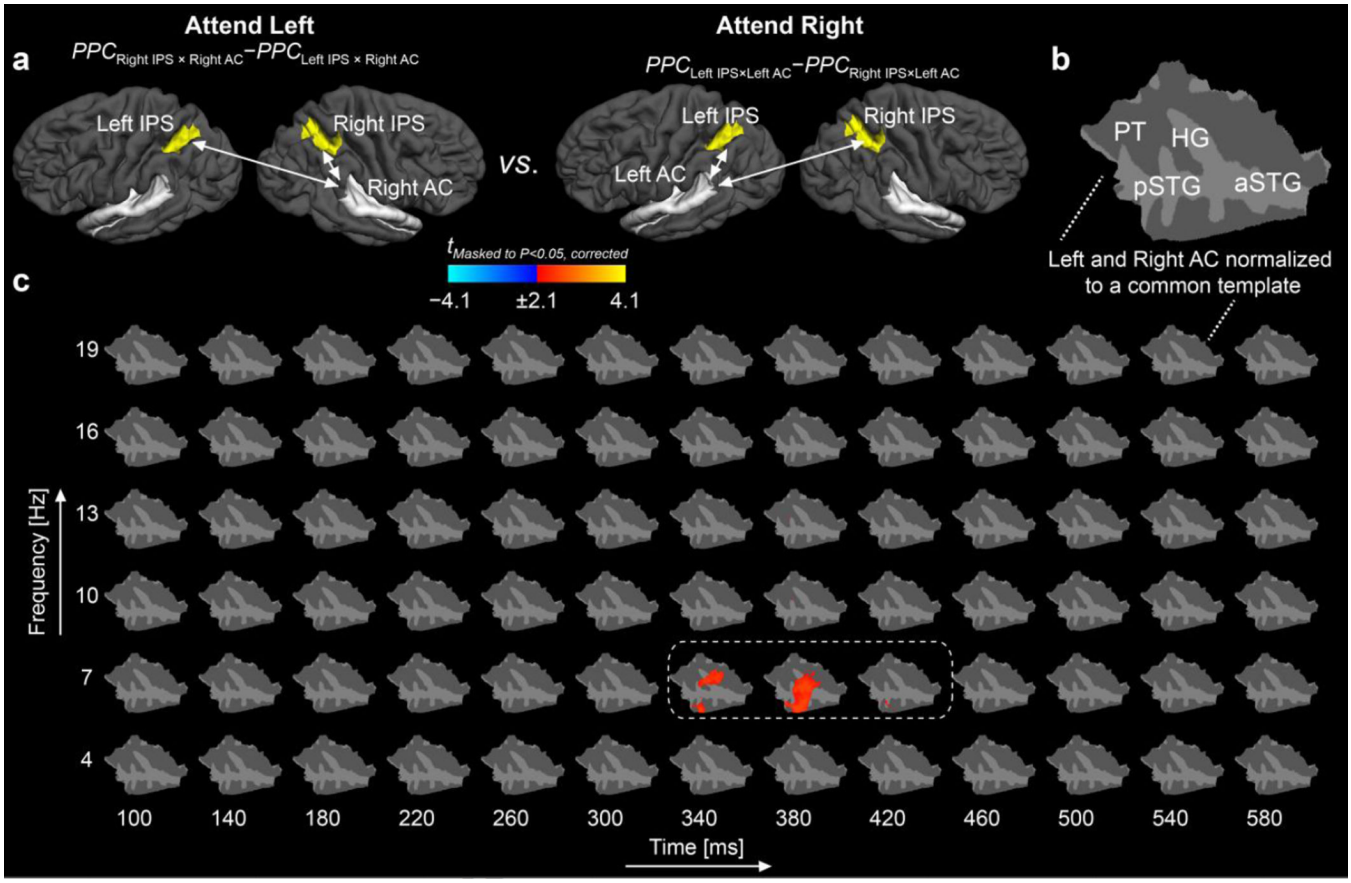

Figure 4.

Factorial analysis on cross-hemispheric phase locking between IPS seeds and AC vertex points during auditory attention. (**a**) The factorial model constructed to normalize out potential baseline differences in left vs. right AC source estimates. For each AC / attention condition, a difference between intra-hemispheric and cross-hemispheric PPC were first calculated, and the resulting vertexby-vertex representations of in the left *vs*. right AC were then compared. (**b**) The left and right AC were co-registered to a common cortical surface template (flattened patch of AC). (**c**) As supporting our hypothesis, the difference between intra- vs. cross-hemispheric phase locking between IPS and AC was stronger in the right than in the left hemisphere when attention was, in each case, directed to the ear contralateral to the AC of interest (t = 0 ms refers to the onsets of post-cue non-target tones). The overall pattern is consistent with the comparison shown in Fig 2. However, the differences peak slightly later and are more clearly restricted to the 7-Hz band (encircled). The figure shows t values masked to locations where the PPC differences were statistically significant (P<0.05, cluster-based randomization test).

Neuroimage. Author manuscript; available in PMC 2015 February 01.

Table 1

Group median ± bootstrapped standard error of the median PPC values between IPS and AC. In each subject, the PPC values pooled across 50–650 ms after attended non-target sound onsets. The *a priori* comparisons reflect Wilcoxon signed rank test between the intra- vs. cross-hemispheric PPC (*p<0.05, **p<0.01). The intra-hemispheric PPC was significantly larger than cross-hemispheric PPC in the right HG, PT, and pSTG, with the differences at 10 Hz being most wide spread. In contrast, in certain the left PT and pSTG, the cross-hemispheric PPC was larger than intra-hemispheric PPC, consistent with the idea that the right IPS dominates auditory spatial attention.

		Attend Left		Attend Right	
AC region	**f [Hz]**	**Right AC × Right IPS**	**Right AC × Left IPS**	**Left AC × Left IPS**	**Left AC × Right IPS**
Heschl's gyrus	4	0.031 ± 0.015	0.021 ± 0.015**	0.037 ± 0.019	0.033 ± 0.011
	7	0.033 ± 0.012	0.017 ± 0.010**	0.019 ± 0.008	0.019 ± 0.006
	10	0.027 ± 0.018	0.024 ± 0.008**	0.049 ± 0.012	0.039 ± 0.013
	13	0.022 ± 0.016	0.022 ± 0.008	0.028 ± 0.008	0.028 ± 0.010
	16	0.017 ± 0.014	0.011 ± 0.006	0.016 ± 0.007	0.007 ± 0.009
	19	0.018 ± 0.014	0.005 ± 0.005**	0.007 ± 0.005	0.005 ± 0.004
Planum temporale	4	0.006 ± 0.006	0.004 ± 0.006*	0.008 ± 0.004	0.001 ± 0.003
	7	0.010 ± 0.005	0.006 ± 0.004	0.010 ± 0.005	0.015 ± 0.006*
	10	0.018 ± 0.009	0.007 ± 0.004*	0.023 ± 0.008	0.016 ± 0.008
	13	0.017 ± 0.006	0.013 ± 0.005	0.024 ± 0.008	0.013 ± 0.008
	16	0.005 ± 0.005	0.004 ± 0.004	0.011 ± 0.008	0.007 ± 0.007
	19	0.006 ± 0.003	0.005 ± 0.002	0.005 ± 0.003	0.006 ± 0.003
Posterior STG	4	0.011 ± 0.009	0.010 ± 0.007	0.011 ± 0.006	0.005 ± 0.003
	7	0.013 ± 0.007	0.012 ± 0.006	0.011 ± 0.004	0.016 ± 0.005*
	10	0.024 ± 0.010	0.008 ± 0.009*	0.037 ± 0.009	0.022 ± 0.009
	13	0.018 ± 0.007	0.014 ± 0.005	0.032 ± 0.011	0.011 ± 0.011
	16	0.008 ± 0.008	0.003 ± 0.004	0.017 ± 0.007	0.008 ± 0.008
	19	0.010 ± 0.006	0.007 ± 0.004*	0.005 ± 0.005	0.004 ± 0.005
Anterior STG	4	0.008 ± 0.004	0.009 ± 0.005	0.006 ± 0.006	0.008 ± 0.005
	7	0.013 ± 0.006	0.007 ± 0.009	0.020 ± 0.008	0.014 ± 0.005
	10	0.023 ± 0.009	0.025 ± 0.007	0.036 ± 0.020	0.027 ± 0.013
	13	0.010 ± 0.006	0.017 ± 0.009	0.018 ± 0.018	0.017 ± 0.012
	16	0.006 ± 0.005	0.007 ± 0.005	0.012 ± 0.008	0.011 ± 0.006
	19	0.006 ± 0.005	0.005 ± 0.004	0.009 ± 0.004	0.009 ± 0.004